Different Photodimerization Behaviour of Tranilast in α-, β- and γ-Cyclodextrin Complexes: Cavity-size and Stoichiometry Dependence

Tadanobu Utsuki, Fumitoshi Hirayama and Kaneto Uekama*
Faculty of Pharmaceutical Sciences, Kumamoto University, 5-1 Oe-honmachi, Kumamoto 862, Japan

The effects of α-, β- and γ-cyclodextrins (CDxs) on the photoisomerization and photodimerization of an antiallergic drug tranilast [**1**, *N*-(3,4-dimethoxycinnamoyl)anthranilic acid] have been kinetically investigated. α- and β-CDxs decelerate both the photoisomerization and photodimerization of **1**, showing saturation kinetics, due to 1:1 complex formation. On the other hand, γ-CDx accelerates the photodimerization of **1** at higher **1**:γ-CDx molar ratios, but decelerates it at lower **1**:γ-CDx molar ratios. The photoisomerization of **1** is decelerated over the γ-CDx concentration range employed. The continuous variation plot of CDx-induced circular dichroism intensities of **1** and the solubility data indicate that **1** forms inclusion complexes with γ-CDx in different stoichiometry, depending on the guest:host molar ratio. At higher **1**:γ-CDx molar ratios, **1** formed the 2:1 (guest:host) complex which accelerates by about 5500 times, the dimerization of **1**. With increasing γ-CDx concentration, 1:1 and 1:2 complexes are formed and the dimerization rate of **1** decreases markedly; in particular, the 1:2 complex decelerates it by 19 300 times. The results reveal clear evidence for the cavity-size- and stoichiometry-dependent dimerization of **1** in CDx complexes.

Cyclodextrins (CDxs) are known to form inclusion complexes with a variety of guest molecules, and inclusion by CDxs shows high size-complementarity between guest and host molecules.[1] For example, α- and β-CDxs form usually 1:1 or 1:2 (guest:host) complexes, because of the relatively small cavity size. On the other hand, γ-CDx has the unique property of including two guest molecules within its large cavity.[2] The size-dependence of the stoichiometry markedly affects the chemical reactivities of guest molecules. As yet, however, clear kinetic evidence on the stoichiometry-dependent reactivity change of guests has been rather scarce, except for a few reports on bimolecular reactions such as Diels–Alder cycloadditions and dimerizations of anthracene.[3]

In a preliminary communication,[4] we reported kinetic evidence that γ-CDx forms inclusion complexes with different stoichiometry, affecting the photodimerization rate of an antiallergic drug tranilast **1** [*N*-(3,4-dimethoxycinnamoyl)anthranilic acid].[5] This paper reports detailed results on the photoreaction of **1** in the γ-CDx complex, in comparison with those in the α- and β-CDx complexes.

Experimental

Kinetic Measurements.—Pyrex tubes containing aqueous solutions of **1** (phosphate buffer, pH 7.0 and μ 0.2 mol dm^{-3}) were set on a merry-go-round type apparatus and the solutions were irradiated at 25 °C with a UV-A lamp (Toshiba FL20SE-30, Tokyo) which emits between 320 and 400 nm with a maximum at 365 nm, the energy intensity being about 0.1 mW cm^{-2} at 365 nm. Concentrations of **1** and its photoproducts, (*Z*)-isomer **2** and dimer **3**, were measured by high performance liquid chromatography (Hitachi 635 A, Tokyo): column, LiChrosorb RP-18; mobile phase, acetonitrile–methanol–0.1 mol dm^{-3} acetic acid (31.5/70/9.5); flow rate, 1.0 cm^3 min^{-1}; internal standard, diazepam; detection, UV monitor at 330 nm.

Measurements of Circular Dichroism (CD) Spectra.—CD spectra were recorded with a Jasco J-50 recording polarimeter at 25 °C, using phosphate buffer (pH 7.0, μ 0.2 mol dm^{-3}).

Solubility Studies.—Solubility measurements were carried out according to the method of Higuchi and Connors.[6] Excess amounts (2 mg) of **1** were added to an aqueous solution (2 cm^3) containing various concentrations of CDxs, and the solutions were shaken at 25 °C in the dark. After equilibrium (about 7 days), an aliquot was centrifuged and pipetted through a cotton plug. The filtrate was diluted with water and analysed spectrophotometrically at 330 nm. The apparent 1:1 association constant, $K_{1:1}$, of the complex was calculated from the slope and intercept of the initial linear portion of the phase-solubility diagram according to eqn. (1).[6]

$$K_{1:1} = \text{slope}/[\text{intercept}\cdot(1 - \text{slope})] \quad (1)$$

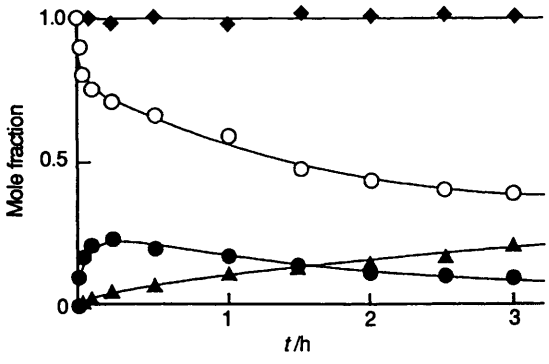

Fig. 1 Photoreaction profiles for: (○) **1**; (●) **2**; (▲) **3** and (◆) total mole fraction of **1**, **2**, and **3**. The initial concentration of **1** was 2.5 × 10^{-5} mol dm^{-3}. Solid curves show the theoretical profiles calculated by using k_1, k_{-1} and k_2 values in the text.

Results and Discussion

Photoreaction of **1**.—Fig. 1 shows the time–conversion plots for the photoreaction of **1**. As the concentration of **1** decreased, the (*Z*)-isomer **2** rose to a maximum and decreased after about 15 min with the formation of the dimer **3**. Under the experimental conditions, no products other than **2** and **3** were obtained (mass balance greater than 98%), suggesting that the photoreaction of **1** proceeds according to Scheme 1. In order to obtain the rate constants (k_{-1}, k_1–k_4), these reaction profiles were analysed according to parallel first- and second-order

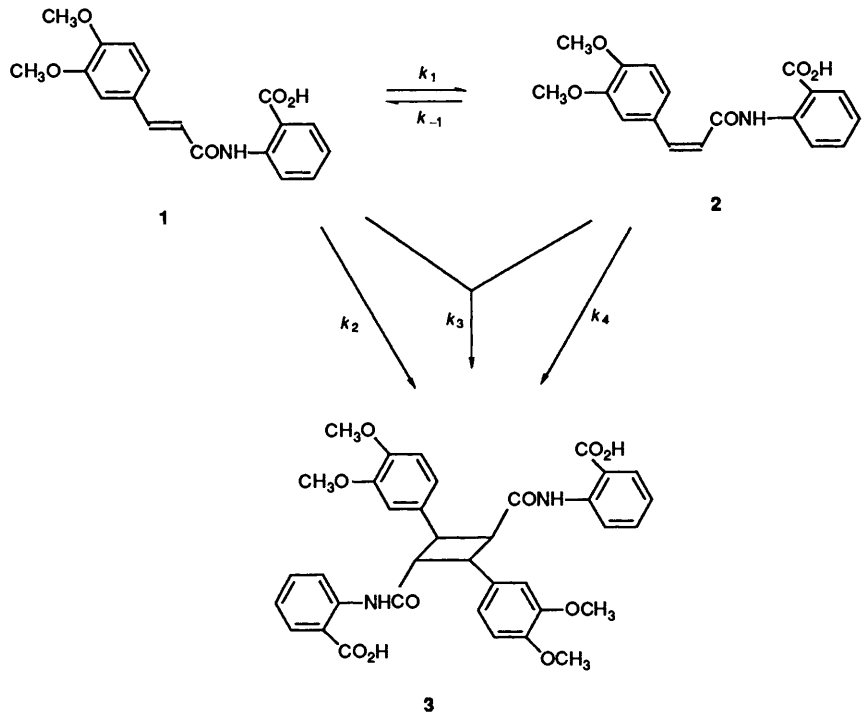

Scheme 1 Photoreaction pathway of **1**

kinetics, eqns. (2)–(4), using a nonlinear least-squares method (MULTI program) in combination with a numerical integration, Runge–Kutta–Gill method.[7]

$$\frac{d[1]}{dt} = -k_1[1] + k_{-1}[2] - k_2[1]^2 - k_3[1][2] \quad (2)$$

$$\frac{d[2]}{dt} = k_1[1] - k_{-1}[2] - k_3[1][2] - k_4[2]^2 \quad (3)$$

$$\frac{d[3]}{dt} = k_2[1]^2 + k_3[1][2] + k_4[2]^2 \quad (4)$$

The results were as follows: $k_1 = 0.17 \pm 0.002$ min^{-1}, $k_{-1} = 0.49 \pm 0.002$ min^{-1}, $k_2 = 1330 \pm 5$ dm^3 mol^{-1} min^{-1}, $k_3 = (1.2 \pm 0.4) \times 10^{-2}$ dm^3 mol^{-1} min^{-1} and $k_4 = (5.4 \pm 0.8) \times 10^{-3}$ dm^3 mol^{-1} min^{-1}. The k_3 and k_4 values were significantly smaller than the k_2 value, indicating that the dimerization of **1** occurs predominantly between two molecules of **1**, but negligibly between two molecules of **2** and between **1** and **2**. Furthermore, there was no concentration-dependence of the rate constants in the range 5×10^{-6}–1×10^{-4} mol dm^{-3} of **1**. The structure of **3** was estimated to be the antihead-to-tail type cyclobutane dimer, by reference to the ^{1}H NMR spectroscopic data,[8] *i.e.*, δ(Ha) = 4.15 and δ(Hb) = 4.50 (internal reference TMS), and J_{ab} = 10.3 and 7.3 Hz for **3**. Because this reaction behaviour of **1** was not changed even in the presence of CDxs, the dimerization pathways of k_3 and k_4 were neglected in the following kinetic treatment.

Effect of CDxs *on the Photoisomerization of* **1**.—Fig. 2 shows the changes in the isomerization rate constants of **1** and **2**, as a function of CDx concentration. The isomerization of **1** and **2** was decelerated by the addition of CDxs, where the α- and β-CDx systems showed typical saturation kinetics. Therefore, the association constant ($K_{1:1}$) and rate constant for **1**•α-CDx and **1**•β-CDx complexes were evaluated from the rate–CDx concentration profile, using eqn. (6),[1a] which follows from the 1:1 complexation [eqn. (5)];

$$\mathbf{1} + \mathrm{CDx} \overset{K_{1:1}}{\rightleftharpoons} \mathbf{1}\cdot\mathrm{CDx} \quad (5)$$

$$k_{obs}^{iso}[\mathbf{1}]_t = k_0^{iso}[\mathbf{1}] + k_c^{iso}[\mathbf{1}\cdot\mathrm{CDx}] \quad (6)$$

where k_{obs}^{iso} is the isomerization rate constant in the presence of CDxs, k_0^{iso} and k_c^{iso} are those of **1** and **1**•CDx complex, respectively, and $[\mathbf{1}]_t$ is the total concentration of **1**. The results are listed in Table 1. The decelerating effect of β-CDx on the isomerization of **1** was greater than that of α-CDx and the binding constant of **1** to CDx was slightly larger than that of the (*Z*)-form. These results were in good agreement with a previous report about the (*E*)–(*Z*) photoisomerization of a cinnamic acid derivative.[9] In the case of the γ-CDx system, on the other hand, the rate deceleration of **1** varied slightly with the host concentration and did not simply obey the saturation kinetics involving the 1:1 complexation. This was attributable to the stoichiometry change of the **1**•γ-CDx complex depending on guest:host molar ratio, as is described later. The quantitative analysis of the rate–γ-CDx concentration profile was difficult because of the small change in the rate.

Effects of CDxs *on the Photodimerization of* **1**.—The photodimerization of **1** showed different dependences on concentration of CDxs (Fig. 3), *i.e.* α- and β-CDxs decelerated it asymptotically, showing saturation kinetics, whereas, γ-CDx accelerated it up to *ca.* 3.0×10^{-5} mol dm^{-3} of γ-CDx, but decelerated it with further increase in γ-CDx concentration. At a constant concentration of γ-CDx (2.5×10^{-5} mol dm^{-3}), the dimerization was decelerated at lower concentrations of **1** ($< 7.0 \times 10^{-6}$ mol dm^{-3}), whereas it was accelerated at higher concentrations of **1** (1.0×10^{-5} mol dm^{-3}). These results suggest that the dimerization rate of **1** is controlled by the stoichiometry of the complexes.

In order to assess the stoichiometry of the **1**•CDx complexes, the continuous variation plots[10] and the phase-solubility plots[6] were made at relatively low and high concentrations of CDx, respectively. Fig. 4 shows the continuous variation plots of ellipticity at 330 nm of the **1**•CDx system. The plots gave

Table 1 Photoisomerization rate constants of **1** and **2** in α- and β-CDx complexes, and their association constants

System	$1 \longrightarrow 2$ k_0^{iso} or k_c^{iso}/min^{-1}	$2 \longrightarrow 1$ k_0^{iso} or k_c^{iso}/min^{-1}	$k_{1:1}$/dm^3 mol^{-1} K_1 [a]	K_2 [b]
1 alone	0.17 ± 0.002	0.49 ± 0.002	—	—
α-CDx complex	0.065 ± 0.003	0.28 ± 0.002	90 ± 15	80 ± 10
β-CDx complex	0.051 ± 0.002	0.16 ± 0.003	220 ± 10	100 ± 20

[a] $K_{1:1}$ of **1**-CDx complex. [b] $K_{1:1}$ of **2**-CDx complex.

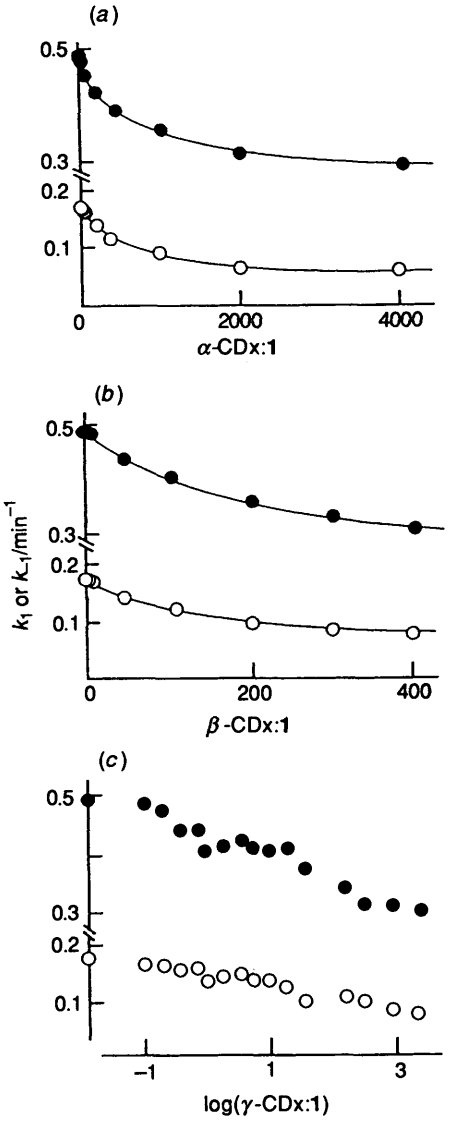

Fig. 2 Photoisomerization rate constants, k_1 (○) and k_{-1} (●), of **1** *vs.* molar ratios of CDxs and **1**: (*a*) α-CDx; (*b*) β-CDx; (*c*) γ-CDx. The initial concentration of **1** was 2.5 × 10^{-5} mol dm^{-3}. Solid curves show the theoretical k_1 and k_{-1} calculated by using eqn. (6) and the rate constants and association constants in Table 1.

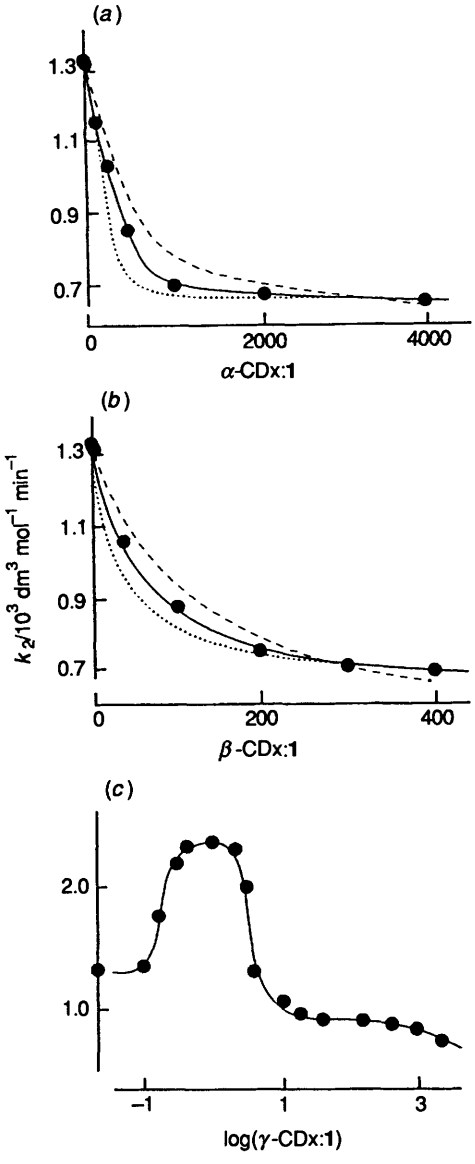

Fig. 3 Photodimerization rate constants k_2 of **1** *vs.* molar ratios of CDxs and **1**: (*a*) α-CDx; (*b*) β-CDx; (*c*) γ-CDx. The initial concentration of **1** was 2.5 × 10^{-5} mol dm^{-3}. Solid curves in (*a*) and (*b*) show the theoretical k_2 calculated by using eqn. (9) and the rate constants and association constants in Table 2. Dotted and broken curves were calculated using eqns. (7) and (8), respectively.

maxima at 0.5, 0.5 and 0.66 for the α-, β- and γ-CDx complexes, indicating 1:1, 1:1 and 2:1 (guest:host) stoichiometries, respectively. Fig. 5 shows the phase-solubility diagrams for the **1**-CDx complexes. The solubility of **1** increased linearly with α- and β-CDx concentrations, showing an A_L type diagram, as defined by Higuchi and Connors,[6] indicating the presence of only one species of the complex. On the other hand, the solubility curve of the γ-CDx system showed a typical B_s type, *i.e.* the solubility of **1** increased linearly at lower γ-CDx concentrations, followed by a plateau region, and decreased at higher concentrations of the host owing to precipitation of the less water-soluble complex. The powder X-ray diffraction pattern of the resulting solid complex was different from that of the physical mixture of **1** and γ-CDx, and the chemical analysis indicated that the solid γ-CDx complex has a 1:2 (guest:host) stoichiometry. This 1:2 stoichiometry was in good agreement

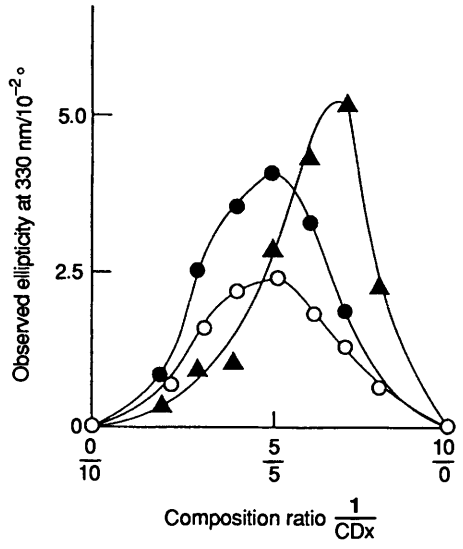

Fig. 4 Changes in ellipticity at 330 nm of **1**•CDx systems in phosphate buffer (pH 7.0 μ 0.2 mol dm^{-3}) at 25 °C, monitored by the continuous variation method: (○) α-CDx; (●) β-CDx; (▲) γ-CDx. The total concentration of **1** and CDxs was 5.0 × 10^{-6} mol dm^{-3}.

with that estimated from the length of the plateau region of the solubility diagram (Fig. 5).[6] These CD spectroscopy and solubility data indicate that **1** forms inclusion complexes with γ-CDx in different stoichiometry, depending on the guest:host concentration ratio, whereas both α- and β-CDxs form only the 1:1 complexes. The association constants of 1:1 complexes ($K_{1:1}$) were determined, using eqn. (1), from the initial straight line of the solubility diagrams at relatively low concentration of CDxs, and were 60 dm^3 mol^{-1}, 160 dm^3 mol^{-1} and 190 dm^3 mol^{-1} for the α, β- and γ-CDx complexes, respectively.

Therefore, the following equilibria and rate equations were considered to interpret the CDx concentration-dependence of the photodimerization (k_2) of **1** (Fig. 3).

(i) For the α- and β-CDx complexes, the rate equations, (7)–(9), were considered on the basis of 1:1 complexation [eqn. (5)], where $[\mathbf{1}]_t$ is the total concentration of **1**, and k_{obs} and k_0 are

$$k_{obs}[\mathbf{1}]_t^2 = k_0[\mathbf{1}]^2 + k_{1:1}[\mathbf{1}][\mathbf{1}\text{•CDx}] \quad (7)$$

$$k_{obs}[\mathbf{1}]_t^2 = k_0[\mathbf{1}]^2 + k'_{1:1}[\mathbf{1}\text{•CDx}]^2 \quad (8)$$

$$k_{obs}[\mathbf{1}]_t^2 = k_0[\mathbf{1}]^2 + k_{1:1}[\mathbf{1}][\mathbf{1}\text{•CDx}] + k'_{1:1}[\mathbf{1}\text{•CDx}]^2 \quad (9)$$

dimerization constants of **1** in the presence and absence of CDxs, respectively. $k_{1:1}$ and $k'_{1:1}$ are the dimerization rate constants of **1** with **1**•CDx and **1**•CDx with **1**•CDx, respectively. Thus, the data of Fig. 3 were analysed by a nonlinear least-squares method,[7] using each eqn. (7)–(9) in combination with eqn. (5). As shown in Fig. 3, the simulated curve using eqn. (9) was most closely fitted with the observed data, whereas neither eqn. (7) nor eqn. (8) was fitted [Akaike information index (AIC)[11] of eqn. (9) was smallest among the three equations: −12.5, −20.2 and −55.5 for eqns. (7)–(9), respectively]. Thus, the dimerization of **1** in the presence of α- or β-CDxs proceeds according to eqn. (9), *i.e.* dimerizations between two molecules of **1** in the free state, between **1**•CDx complex and **1**, and between two **1**•CDx complexes. The term, $k'_{1:1}[\mathbf{1}\text{•CDx}]^2$, in eqns. (8) and (9) is kinetically equivalent to the rate equation, $k_{2:2}$•$K_{2:2}[\mathbf{1}_2\text{•CDx}_2]$, for the 2:2 complex, where $k_{2:2}$ and $K_{2:2}$ are the dimerization rate constant of **1** in the 2:2 complex and the association constant of the 2:2 complex, respectively. However, formation of the 2:2 complex was negligible for the

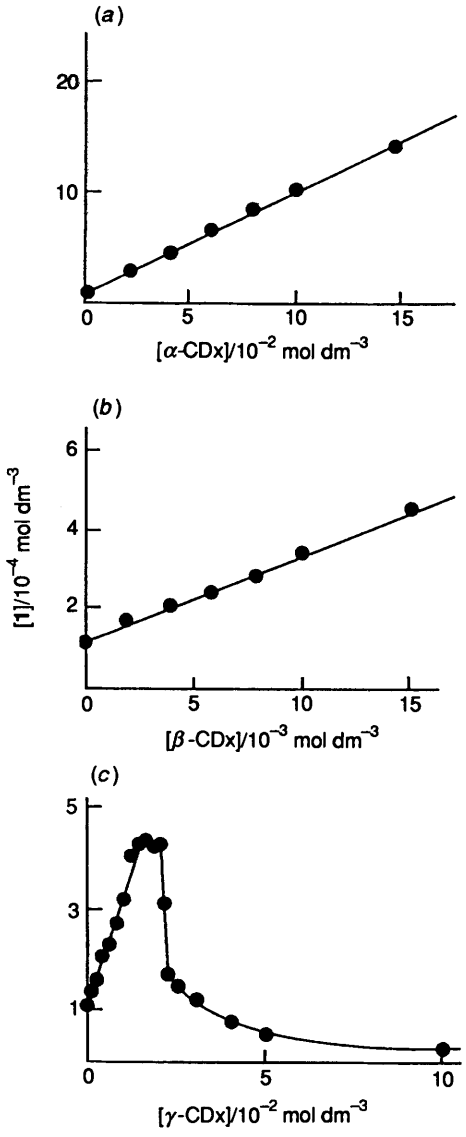

Fig. 5 Phase-solubility diagrams of **1**•CDx systems in phosphate buffer (pH 7.0, μ 0.2 mol dm^{-3}) at 25 °C; (*a*) α-CDx; (*b*) β-CDx; (*c*) γ-CDx

following reasons. (1) If the 2:2 complex is formed, the dimerization should be accelerated due to a close contact of two molecules of **1**, as observed in the γ-CDx complex (which will be described later). (2) If the 2:2 complex is formed, the dimerization rate should change in more alkaline media (pH > 11) because the 2:2 complex dissociates to the 1:1 complex owing to the electrostatic repulsion between negatively charged hydroxy groups of CDxs (p*Ka* *ca.* 12).[12] Such dissociation of a 2:2 complex to a 1:1 complex was demonstrated spectrophotometrically by Ueno *et al.*[13] and Hamai.[14] However, as shown in Fig. 6, no pH-dependence of the dimerization rates in the absence and even presence of α- and β-CDxs was observed. The kinetic parameters and association constants determined according to eqn. (9) are listed in Table 2. The $k_{1:1}$ value was slightly smaller than the k_0 value, suggesting that the access of one more **1** to the 1:1 complex may not be severely hindered owing to the only partial inclusion, as is apparent from the smaller $K_{1:1}$ value. On the other hand, the $k'_{1:1}$ values were about one-half the k_0 value, indicating that an orientation of two **1**•CDx complexes favourable for the dimerization is sterically hindered.

(ii) For the γ-CDx complex, the following equilibria and rate equation [3b,15] [eqns. (10)–(13)] were considered on the basis of

Table 2 Photodimerization rate constants of **1** in CDx complexes and their association constants

System	k_0[a]	$k_{1:1}$[a]	$k'_{1:1}$[a]	$k_{2:1}$[b]	$k_{1:2}$[a]	$K_{1:1}$[c]	$K_{2:1}$[c]	$K_{1:2}$[c]
1 alone	1330 ± 4	—	—	—	—	—	—	—
α-CDx complex	—	1160 ± 10	690 ± 30	—	—	60 ± 20	—	—
β-CDx complex	—	1170 ± 20	560 ± 20	—	—	220 ± 15	—	—
γ-CDx complex	—	1040 ± 20	630 ± 40	3310 ± 70	(6.9 ± 0.8) × 10^{-2}	200 ± 20	2210 ± 90	1160 ± 40

[a] $dm^3\ mol^{-1}\ min^{-1}$. [b] min^{-1}. [c] $dm^3\ mol^{-1}$.

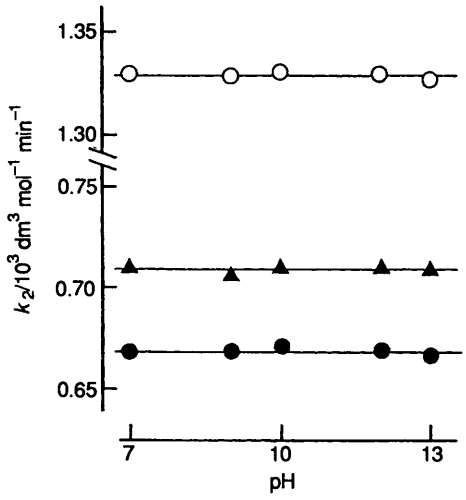

Fig. 6 pH profiles for photodimerization rate constants k_2 in the absence (○) and presence of α-CDx (●, 0.1 mol dm^{-3}) and β-CDx (▲, 0.01 mol dm^{-3})

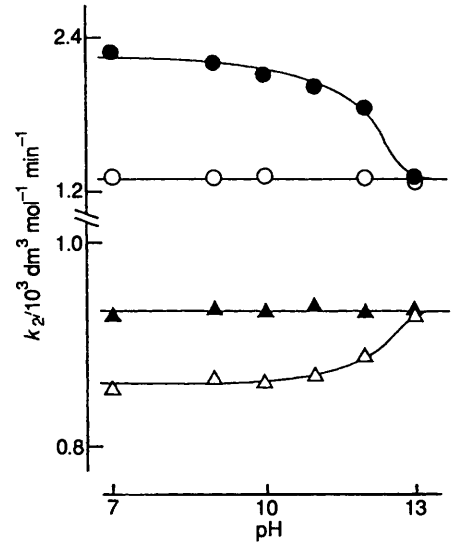

Fig. 7 pH profiles for photodimerization rate constants k_2 in the absence (○) and presence of γ-CDx, (●) 1.0 × 10^{-5} mol dm^{-3}; (▲) 1.0 × 10^{-3} mol dm^{-3} and (△) 2.0 × 10^{-2} mol dm^{-3}

the results of the continuous variation plots and the solubility data.

$$\mathbf{1} + \gamma\text{-CDx} \overset{K_{1:1}}{\rightleftharpoons} \mathbf{1}\cdot\gamma\text{-CDx} \quad (10)$$

$$\mathbf{1}\cdot\gamma\text{-CDx} + \mathbf{1} \overset{K_{2:1}}{\rightleftharpoons} \mathbf{1}_2\cdot\gamma\text{-CDx} \quad (11)$$

$$\mathbf{1}\cdot\gamma\text{-CDx} + \gamma\text{-CDx} \overset{K_{1:2}}{\rightleftharpoons} \mathbf{1}\cdot(\gamma\text{-CDx})_2 \quad (12)$$

$$k_{obs}[\mathbf{1}]_t^2 = k_0[\mathbf{1}]^2 + k_{1:1}[\mathbf{1}][\mathbf{1}\cdot\gamma\text{-CDx}] + k'_{1:1}[\mathbf{1}\cdot\gamma\text{-CDx}]^2 + k_{2:1}[\mathbf{1}_2\cdot\gamma\text{-CDx}] + k_{1:2}[\mathbf{1}][\mathbf{1}\cdot(\gamma\text{-CDx})_2] \quad (13)$$

$k_{2:1}$ and $k_{1:2}$ are dimerization rate constants of $\mathbf{1}_2$·γ-CDx and **1**·(γ-CDx)$_2$ with **1**, respectively, and $K_{2:1}$ and $K_{1:2}$ are association constants of the 2:1 and 1:2 complexes, respectively. Reactions higher than third-order with respect to **1** were not considered, because of a low probability in chemical reactions.[16]

In order to determine whether the third term of eqn. (13) is due to the reaction of two **1**·γ-CDx complexes, $k'_{1:1}[\mathbf{1}\cdot\gamma\text{-CDx}]^2$, or to that of the 2:2 complex, $k_{2:2}\cdot K_{2:2}[\mathbf{1}_2\cdot(\gamma\text{-CDx})_2]$, the pH-dependence of the dimerization rates in the absence and presence of γ-CDx was investigated. Fig. 7 shows the pH profiles of the dimerization rate of **1** in the absence and presence of γ-CDxs at concentrations of 1 × 10^{-5} mol dm^{-3}, 1 × 10^{-3} mol dm^{-3} and 2 × 10^{-2} mol dm^{-3}, where the 2:1, 1:1 or 2:2 and 1:2 complexes, respectively, are predominantly formed. The dimerization rates of **1** in the absence of CDx (corresponding to k_0) and in the presence of 1 × 10^{-3} mol dm^{-3} γ-CDx (corresponding to $k_{1:1}$, $k'_{1:1}$ or $k_{2:2}$) were little affected by the pH change from 7 to 13, indicating negligible formation of the 2:2 complex. On the other hand, the dimerization rate in the presence of 2 × 10^{-2} mol dm^{-3} γ-CDx (corresponding to $k_{1:2}$) increased and approached the $k_{1:1}$ or $k'_{1:1}$ value at pH > 11. This result indicates that in the high pH region, the **1**·(γ-CDx)$_2$ complex dissociates to the 1:1 complex because of the electrostatic repulsion of the secondary hydroxy groups of γ-CDx, thus $k_{1:2}$ approaches $k_{1:1}$ or $k'_{1:1}$. In the case of the low γ-CDx concentration (1 × 10^{-5} mol dm^{-3}), the dimerization rate (corresponding to $k_{2:1}$) decreased and approached the k_0 value at pH > 11. In this case, $k_{2:1}$ did not approach $k_{1:1}$ or $k'_{1:1}$, which may be ascribed to the dissociation of the $\mathbf{1}_2$·γ-CDx complex (2:1) to the **1**·γ-CDx complex (1:1) due to the electrostatic repulsion between the negatively charged host and two guests. However, at such low concentrations of γ-CDx (1 × 10^{-5} mol dm^{-3} where the 2:1 complex is predominantly formed), $k_{2:1}$ did not decrease to the $k_{1:1}$ or $k'_{1:1}$ due to the low concentration of the 1:1 complex. Indeed, the analysis of the $k_{1:2}$, and $k_{2:1}$, pH profiles gave a p*K*a of 12.5 for the hydroxy group of γ-CDx, which agreed with the reported value.[12] The rate constants and association constants, optimized by using eqn. (13), are listed in Table 2. The association constants ($K_{1:1}$) of the 1:1 complexes were in good agreement with those determined from the isomerization rates of **1** and from the solubility data. The dimerization-reactivity of **1** in the 1:1 γ-CDx complex was almost the same as those in the α- and β-CDx complexes. The dimerization of **1** was markedly accelerated by formation of the 2:1 complex, whereas it was decelerated by formation of the 1:2 complex. For example, when the rate constant is compared in second-order dimension, the dimerization rate in the $\mathbf{1}_2$·γ-CDx complex is faster by about 5500 and 7030 times than those for free **1** and **1**·γ-CDx complex, respectively ($k_{2:1} \times K_{2:1}$ = 7.32 × 10^6 $dm^3\ mol^{-1}\ min^{-1}$, k_0 = 1330 $dm^3\ mol^{-1}\ min^{-1}$, $k_{1:1}$ = 1040 $dm^3\ mol^{-1}\ min^{-1}$ and $k'_{1:1}$ = 630 $dm^3\ mol^{-1}\ min^{-1}$). On the other hand, the

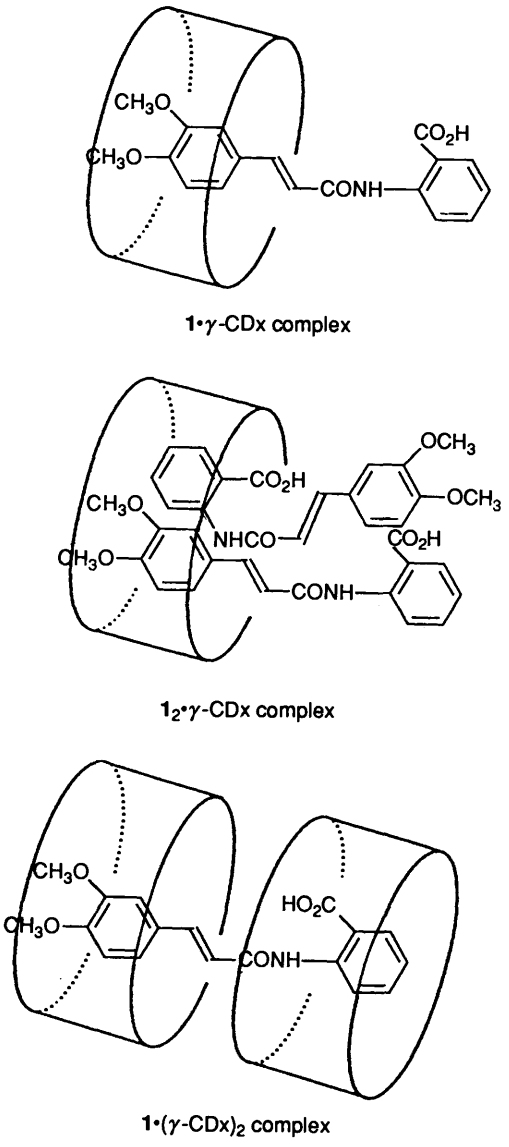

Fig. 8 Proposed inclusion modes of 1–γ-CDx complexes

dimerization rate of **1** in the **1**•(γ-CDX)$_2$ complex was slower by about 19 300 times than that of free **1** (k_0 = 1330 dm^3 mol^{-1} min^{-1} and $k_{1:2}$ = 6.9 × 10^{-2} dm^3 mol^{-1} min^{-1}).

Fig. 8 shows inclusion modes of the three complexes of **1** with γ-CDx, estimated from the above-mentioned kinetic results, together with space-filling molecular models. At higher **1**:γ-CDx molar ratios, two molecules of **1** are included in the γ-CDx cavity in a head-to-tail mode favourable for the dimerization, leading to the marked acceleration. With increasing γ-CDx concentration, one molecule of **1** is withdrawn from the 2:1 complex to form the 1:1 complex, which still retains the dimerization reactivity because of the partial inclusion. Similar 1:1 complexation and reactivity change were observed for the α- and β-CDx complexes. At lower **1**:γ-CDx molar ratios, **1** is completely included by two γ-CDxs and its photoreactivity is lost because of the inaccessibility of the 1:2 complex to another molecule of **1**, resulting in the 19 300-fold deceleration.

In this study, we have demonstrated clearly that the cavity size of CDxs and the stoichiometry change of the complex markedly affect the photodimerization of **1**, and guest:host molar ratios may have to be optimized to achieve maximal acceleration or deceleration for other dimerizing systems of CDx complexes, particularly for γ-CDx which has a large cavity size.

References

1 (*a*) M. L. Bender and M. Komiyama, *Cyclodextrin Chemistry*, Springer-Verlag, Berlin, 1977; (*b*) J. Szejtli, *Cyclodextrins and Their Inclusion Complexes*, Akadémiai Kiadó, Budapest, 1982; (*c*) W. Saenger, *Angew. Chem., Int. Ed. Engl.*, 1980, **21**, 344.
2 F. Hirayama and K. Uekama in *Cyclodextrins and Their Industrial Uses*, ed. D. Duchêne, Editions de Santé, Paris, 1987, p. 131.
3 (*a*) D. C. Rideout and R. Breslow, *J. Am. Chem. Soc.*, 1980, **102**, 7818; (*b*) H.-J. Schneider and N. K. Sangwan, *J. Chem. Soc., Perkin Trans. 2*, 1989, 1223; (*c*) D. L. Wernick, A. Yazbek and J. Levy, *J. Chem. Soc., Chem. Commun.*, 1990, 956.
4 F. Hirayama, T. Utsuki and K. Uekama, *J. Chem. Soc., Chem. Commun.*, 1991, 887.
5 H. Azuma, K. Banno and Y. Yoshimura, *Brit. J. Pharmacol.*, 1976, **58**, 483.
6 T. Higuchi and K. A. Connors, *Adv. Anal. Chem. Instrum.*, 1965, **4**, 117.
7 (*a*) K. Yamaoka, Y. Tanigawara, T. Nakagawa and T. Uno, *J. Pharm. Dyn.*, 1981, **4**, 879; (*b*) K. Yamaoka and T. Nakagawa, *J. Pharm. Dyn.*, 1983, **6**, 595.
8 C. H. Krauch, S. Farid and G. O. Schenck, *Chem. Ber.*, 1966, **99**, 625.
9 F. Hirayama, T. Utsuki, K. Uekama, M. Yamasaki and K. Harata, *J. Pharm. Sci.*, 1992, **81**, 817.
10 P. Job, *Ann. Chem.*, 1928, **9**, 113.
11 H. Akaike, *IEEE Trans. Automat. Contr.*, 1974, **19**, 716.
12 R. L. VanEtten, G. A. Clowes, J. F. Sebastian and M. L. Bender, *J. Am. Chem. Soc.*, 1967, **89**, 3253.
13 A. Ueno, I. Suzuki and T. Osa, *J. Am. Chem. Soc.*, 1989, **111**, 6391.
14 S. Hamai, *J. Phys. Chem.*, 1989, **93**, 6527.
15 K. Kano, I. Takenoshita and T. Ogawa, *Chem. Lett.*, 1982, 321.
16 A. A. Frost and R. G. Pearson, *Kinetics and Mechanism*, John Wiley & Sons, New York, 1961.

Paper 2/03214G
Received 18*th June* 1992
Accepted 29*th September* 1992